

Simulation of $4d \mathcal{N} = 1$ supersymmetric Yang-Mills theory with Symanzik improved gauge action and stout smearing

K. Demmouche^a, F. Farchioni^a, A. Ferling^a, I. Montvay^b,
G. Münster^{a*}, E.E. Scholz^c, J. Wuilloud^a

^a Universität Münster, Institut für Theoretische Physik,
Wilhelm-Klemm-Str. 9, D-48149 Münster, Germany

^b Deutsches Elektronen-Synchrotron DESY, Notkestr. 85, D-22603 Hamburg, Germany

^c Universität Regensburg, Institut für Theoretische Physik,
Universitätsstr. 31, D-93040 Regensburg, Germany

March 10, 2010

Abstract

We report on the results of a numerical simulation concerning the low-lying spectrum of four-dimensional $\mathcal{N} = 1$ SU(2) Supersymmetric Yang-Mills (SYM) theory on the lattice with light dynamical gluinos. In the gauge sector the tree-level Symanzik improved gauge action is used, while we use the Wilson formulation in the fermion sector with stout smearing of the gauge links in the Wilson-Dirac operator. The ensembles of gauge configurations were produced with the Two-Step Polynomial Hybrid Monte Carlo (TS-PHMC) updating algorithm. We performed simulations on large lattices up to a size of $24^3 \cdot 48$ at $\beta = 1.6$. Using QCD units with the Sommer scale being set to $r_0 = 0.5$ fm, the lattice spacing is about $a \simeq 0.09$ fm, and the spatial extent of the lattice corresponds to 2.1 fm. At the lightest simulated gluino mass the spin-1/2 gluino-gluon bound state appeared to be considerably heavier than its expected super-partner, the pseudoscalar bound state. Whether supermultiplets are formed remains to be studied in upcoming simulations.

*email: munsteg@uni-muenster.de

1 Introduction

In recent years supersymmetric theories have aroused increasing interest in elementary particle physics. The supersymmetric extension of the Standard Model with $\mathcal{N} = 1$ supercharge is considered to be an interesting candidate for a quantum field theory with phenomenological relevance in the near future. Supersymmetry (SUSY) is an essential ingredient also for other models beyond the Standard Model.

The $\mathcal{N} = 1$ Supersymmetric Yang-Mills (SYM) theory is the minimal supersymmetric extension of the $SU(N_c)$ gauge theory describing self-interactions of gauge fields A_μ^a , corresponding to the *gluons* (g). The supersymmetric partners of the gluons are described by spin-1/2 Majorana fermion fields λ^a ($a = 1, \dots, N_c^2 - 1$), the *gluinos* (\tilde{g}). Compatibility of SUSY with gauge invariance requires that the gluinos transform in the adjoint representation of the gauge group. This theory describes the interactions between gluons and gluinos. The Lagrangian of Euclidean SYM theory in the continuum, including a SUSY breaking mass term, reads

$$\mathcal{L}_{\text{SYM}} = \frac{1}{4} F_{\mu\nu}^a F_{\mu\nu}^a + \frac{1}{2} \bar{\lambda}^a \gamma_\mu (\mathcal{D}_\mu \lambda)^a + \frac{m_{\tilde{g}}}{2} \bar{\lambda}^a \lambda^a, \quad (1)$$

where \mathcal{D}_μ denotes the gauge covariant derivative in the adjoint representation. The gluino mass term introduces a soft breaking of supersymmetry.

In the low-energy regime the interactions become strong. Arguments based on the low-energy effective Lagrangian approach [1, 2] predict the occurrence of non-perturbative dynamics like confinement and spontaneous chiral symmetry breaking in SUSY gauge theories. Confinement is realised by colourless bound states. Since both gluons and gluinos transform according to the adjoint representation, bound states can be built by any number of at least two gluons and gluinos. In the case where the last term in Eq. (1) is switched off ($m_{\tilde{g}} = 0$), an anomalous global chiral symmetry $U(1)_\lambda$ is present. This symmetry is equivalent to the R -symmetry in supersymmetric models. The anomaly does not break the global chiral symmetry completely and a discrete subgroup Z_{2N_c} remains. As in the case of QCD, the discrete chiral symmetry is expected to be spontaneously broken to Z_2 by the non-vanishing value of the gluino condensate $\langle \bar{\lambda} \lambda \rangle$. The consequence of this spontaneous breaking is the existence of N_c degenerate ground states with different orientations of the gluino condensate.

SYM is also equivalent to QCD with a single quark flavour ($N_f = 1$ QCD) in the limit of a large number of colours ($N_c \rightarrow \infty$), where the Majorana spinor is replaced by a single Dirac spinor in the antisymmetric representation of the gauge group [3]. The latter model is also object of investigation by our collaboration [4].

Since confinement occurs in low-energy SYM, standard analytical methods like perturbation theory fail and non-perturbative methods are required. This motivates the introduction of the lattice formulation of SYM. The first lattice formulation of SYM suitable for numerical simulations has been proposed by Curci and Veneziano [5]. It is based on the Wilson discretisation, which proved to be successful in lattice QCD computations in spite of its known limitations. First non-perturbative investigations of SYM on the lattice using this formulation have been performed by [6] in the quenched approximation, and by the DESY-Münster-Roma collaboration with dynamical fermions; see Ref. [7] for

a review, and references [8, 9, 10, 11, 12]. SUSY is broken explicitly by the lattice discretisation. Additionally, in the Wilson approach the mass term and the Wilson-term break both chirality and SUSY explicitly. Both symmetries are expected to be recovered in the continuum limit by tuning the relevant bare mass term to its critical value corresponding to a massless gluino ($m_{\tilde{g}} = 0$), and the gauge coupling towards zero.

In recent years, simulations of $\mathcal{N} = 1$ SYM on the lattice using Ginsparg-Wilson fermions with good chiral properties, such as domain wall fermions, have been initiated [13, 14, 15, 16]. For large lattice volumes and small lattice spacings these formulations require, however, a significantly larger amount of computing resources than the Wilson formulation. The gain of no need for tuning the position of the zero gluino mass point does not compensate by far the advantage of Wilson fermions.

In the past, investigations of the gluino dynamics have been performed using the Two-Step Multi Bosonic (TSMB) algorithm [17]. This algorithm was developed in the framework of the DESY-Münster collaboration. Recently, the Two-Step Polynomial Hybrid Monte Carlo (TS-PHMC) algorithm [18] has been developed and implemented for SYM. This algorithm offers more efficiency and improvements compared to the TSMB algorithm and allows us to collect higher statistics and to simulate small gluino masses $m_{\tilde{g}}$ in this study. Furthermore, due to available computer resources we simulated the theory on volumes with extension larger than 2 fm, which is expected to be the minimally required volume for spectroscopic studies.

The main purpose of this work is to continue the project of the DESY-Münster collaboration for the simulation of $\mathcal{N} = 1$ SU(2) SYM. We present new accurate results obtained with the newly used TS-PHMC algorithm and improved actions.

The most important characteristics of the theory is the mass spectrum of bound states, for which the low-energy effective theories predict a reorganisation of the masses in two massive Wess-Zumino supermultiplets at the SUSY point [1, 2], where the soft breaking vanishes. The introduction of a small gluino mass removes the mass degeneracy between the supermultiplet members. In the lower supermultiplet the ordering of the states with increasing mass is: scalar glueball 0^{++} , spin-1/2 gluino-glueball (χ_L), pseudoscalar glueball 0^{-+} . The ordering is reversed in the higher supermultiplet which contains: adjoint pseudoscalar meson $a\text{-}\eta'$, spin-1/2 gluino-glueball (χ_H), adjoint scalar meson $a\text{-}f_0$.

The plan of this paper is as follows: in the next Section we review the lattice formulation and describe the simulation details. Section 3 is devoted to the static quark potential and the determination of the scale. Methods for the determination of the masses of bound states are described in Section 4. In Section 5 the results on the spectrum are collected and discussed. Finally, we conclude our findings in Section 6.

2 Lattice formulation of $\mathcal{N} = 1$ SYM theory

The Curci-Veneziano action of $\mathcal{N} = 1$ SU(2) SYM theory on a lattice, $S = S_g + S_{\tilde{g}}$, contains the usual plaquette gauge field action S_g , and a fermionic action $S_{\tilde{g}}$ for the gluino. The gauge action S_g can be extended to a more general form which includes, besides the usual (1×1) Wilson loop plaquette term, (1×2) Wilson loops of perimeter six. We employ the *tree-level improved Symanzik* (tlSym) gauge action, given for SU(N_c)

colour group by

$$S_g^{\text{tlSym}} = \beta \sum_x \left(c_0 \sum_{\mu < \nu; \mu, \nu=1}^4 \left\{ 1 - \frac{1}{N_c} \text{Re} U_{x\mu\nu}^{1 \times 1} \right\} + c_1 \sum_{\mu \neq \nu; \mu, \nu=1}^4 \left\{ 1 - \frac{1}{N_c} \text{Re} U_{x\mu\nu}^{1 \times 2} \right\} \right), \quad (2)$$

with the normalisation condition $c_0 = 1 - 8c_1$. The bare gauge coupling g_0 is related to the lattice parameter β by the usual relation $\beta = 2N_c/g_0^2$. For the tlSym action we have $c_1 = -1/12$ [19].

The gluinos are represented by Majorana fermions λ^a in the adjoint representation. They satisfy the Majorana condition

$$\lambda = \lambda^c = \mathcal{C} \bar{\lambda}^T, \quad (3)$$

where $\mathcal{C} = \gamma_0 \gamma_2$ is the charge conjugation matrix in the spinorial representation.

In the gluino sector, the Wilson formulation for fermions proposed in [5] introduces the Wilson term proportional to r , which is an irrelevant term in the continuum limit. We set the Wilson parameter to $r = 1$. The fermion part $S_{\bar{g}}$ of the action is then given by

$$S_{\bar{g}} = \frac{1}{2} \sum_x \bar{\lambda}(x) \lambda(x) - \frac{\kappa}{2} \sum_x \sum_{\mu} [\bar{\lambda}(x + \hat{\mu}) V_{\mu}(x) (1 + \gamma_{\mu}) \lambda(x) + \bar{\lambda}(x) V_{\mu}^T(x) (1 - \gamma_{\mu}) \lambda(x + \hat{\mu})], \quad (4)$$

where κ is the bare hopping parameter which encodes the bare gluino mass $\kappa = (2m_{\bar{g},0} + 8)^{-1}$. The real orthogonal matrices $V_{\mu}(x)$ are the gauge links in the adjoint representation:

$$[V_{\mu}(x)]^{ab} \equiv 2\text{Tr}[U_{\mu}^{\dagger}(x) T^a U_{\mu}(x) T^b] = [V_{\mu}^*(x)]^{ab} = [V_{\mu}^{-1}(x)]^{ba}, \quad (5)$$

where T^a are the generators of $\text{SU}(N_c)$ satisfying $2\text{Tr}(T^a T^b) = \delta^{ab}$. In case of $\text{SU}(2)$ one has $T^a = \frac{1}{2} \sigma^a$ with the Pauli matrices σ^a .

The links $U_{x,\mu}$ in the fermion action can be replaced by *stout*-smeared links [20]. This has the advantage that short range topological defects of the gauge field and the corresponding small eigenvalues of the fermion matrix are removed. Both the tlSym gauge action and the stout smeared links in the fermionic part of the lattice action are introduced in order to accelerate the approach to the continuum limit as $\beta \rightarrow \infty$.

The stout smeared links are defined by

$$U_{x,\mu}^{(1)} \equiv U_{x,\mu} \exp \left\{ \frac{1}{2} (\Omega_{x,\mu} - \Omega_{x,\mu}^{\dagger}) - \frac{1}{2N_c} \text{Tr} (\Omega_{x,\mu} - \Omega_{x,\mu}^{\dagger}) \right\}. \quad (6)$$

Here $U_{x,\mu}$ denotes the original “thin” gauge links, and

$$\Omega_{x,\mu} \equiv \rho U_{x,\mu}^{\dagger} C_{x,\mu} \quad (7)$$

with the sum of “staples”

$$C_{x,\mu} \equiv \sum_{\nu \neq \mu} \left(U_{x+\hat{\mu},\nu}^{\dagger} U_{x+\hat{\nu},\mu} U_{x,\nu} + U_{x-\hat{\nu}+\hat{\mu},\nu} U_{x-\hat{\nu},\mu} U_{x-\hat{\nu},\nu}^{\dagger} \right). \quad (8)$$

ρ is an arbitrary parameter which we fix in this work to $\rho = 0.15$. In principle, the smearing defined by the above equations can be iterated several times, but then the fermion action becomes extended over a larger region on the lattice. We prefer to keep the action well localised and hence only perform a single smearing step.

Writing the gluino action as

$$S_{\tilde{g}} = \frac{1}{2} \sum_{xy} a^4 \bar{\lambda}_y Q_{yx} \lambda_x, \quad (9)$$

Q is the non-hermitian fermion matrix or lattice Wilson-Dirac operator for Dirac fermions in the adjoint representation. Using relation (3), the fermion action can be rewritten in terms of the antisymmetric matrix $M = \mathcal{C}Q$. Integration of the fermionic variables yields the Pfaffian of M ,

$$\int \mathcal{D}\lambda e^{-S_{\tilde{g}}} = \text{Pf}(M), \quad (10)$$

whose absolute value equals the square root of the fermion determinant:

$$|\text{Pf}(M)| = \sqrt{\det(M)} = \sqrt{\det(Q)}. \quad (11)$$

Effectively, this corresponds to a flavour number $N_f = 1/2$. In the Wilson setup, $\det(Q)$ and $\det(M)$ are always real and positive, but the Pfaffian $\text{Pf}(M)$ can become negative even for positive gluino masses.

In our numerical simulations we include the dynamics of the gluino by the Two-Step Polynomial Hybrid Monte Carlo (TS-PHMC) [18] algorithm with flavour number $N_f = 1/2$. This has the consequence that only the absolute value of the Pfaffian is taken into account in the updating of the gauge field configuration. The sign of the Pfaffian has to be included in a reweighting step when calculating expectation values. It can be shown that the sign of the Pfaffian is equal to the sign of the product of half of the doubly degenerate negative real eigenvalues of Q . For positive gluino masses sufficiently far away from zero, a negative sign of the Pfaffian rarely occurs in the updating sequence and therefore in this situation a sign problem does not show up. Approaching the limit of vanishing gluino mass we monitor the sign of the Pfaffian and take it into account by reweighting. It turned out that only in our runs D and D_s (see Table 1 below) a noticeable number of configurations with negative sign occurred; the highest fraction being in point D_s , where they amount to 3% of all configurations. The effect of the negative signs on the particle masses turned out to be negligible.

The parameters of the $\mathcal{N} = 1$ SYM on the lattice are the lattice gauge coupling β and the fermionic hopping parameter κ . Similarly to QCD, the mass term proportional to $m_{\tilde{g},0}$ breaks chirality explicitly. In the present case it also breaks the supersymmetry. A massless gluino, $m_{\tilde{g}} = 0$, is obtained by tuning the bare mass term to its critical value ($m_{\tilde{g},0} \rightarrow m_c$) or equivalently $\kappa \rightarrow \kappa_c$.

In order to study questions related to supersymmetry, one has to approach the critical value of the hopping parameter $\kappa = \kappa_c$ corresponding to zero gluino mass. This tuning problem can be solved rather easily by means of the adjoint pion mass m_π . This is the pion mass in the corresponding theory with two Majorana fermions in the adjoint representation. It is obtained from the exponential decay of the connected part of the

Table 1: *Algorithmic parameters for TS-PHMC runs with tSym gauge action at $\beta = 1.6$. Runs labelled with subscript s have been performed with Stout-links. N_{conf} is the number of configurations produced, r_0 is the Sommer scale parameter, am_π is the adjoint pion mass in lattice units, and M_r is the dimensionless quantity $M_r \equiv (r_0 m_\pi)^2$ used to estimate the gluino mass. In M_r the values of r_0/a extrapolated to κ_c have been used.*

Run	$L^3 \cdot T$	β	κ	N_{conf}	r_0/a	am_π	M_r
A	$16^3 \cdot 32$	1.6	0.1800	2500	2.9(1)	1.3087(12)	45.6(4.2)
B	$16^3 \cdot 32$	1.6	0.1900	2700	3.3(1)	1.0071(12)	27.0(2.5)
C	$16^3 \cdot 32$	1.6	0.2000	10847	4.242(87)	0.5008(13)	6.68(62)
D	$16^3 \cdot 32$	1.6	0.2020	6947	5.04(26)	0.221(12)	1.30(19)
\bar{A}	$24^3 \cdot 48$	1.6	0.1980	1480	3.885(63)	0.6415(13)	11.0(1.0)
\bar{B}	$24^3 \cdot 48$	1.6	0.1990	1400	4.16(12)	0.5759(17)	8.83(82)
\bar{C}	$24^3 \cdot 48$	1.6	0.2000	6465	4.33(19)	0.4947(13)	6.52(61)
A_s	$24^3 \cdot 48$	1.6	0.1500	370		0.9469(38)	28.69(89)
B_s	$24^3 \cdot 48$	1.6	0.1550	1730	4.324(39)	0.5788(16)	10.72(33)
C_s	$24^3 \cdot 48$	1.6	0.1570	2110	5.165(88)	0.3264(23)	3.41(11)
D_s	$24^3 \cdot 48$	1.6	0.1575	2260	5.561(99)	0.2015(93)	1.30(13)

pseudoscalar meson propagator, see below. The pion is not a physical particle in the spectrum of the SYM theory, but it can be unambiguously defined in a partially quenched framework. To determine the pion mass is rather easy, in fact it is the easiest mass to determine. As will be detailed in Sec. 4.4, the behaviour of the pion mass-squared is very closely linear as a function of $1/\kappa$ in the entire range of gluino masses of interest. On the basis of arguments involving the OZI-approximation of SYM [1], the adjoint pion mass is expected to vanish for a massless gluino. Therefore it is enough to perform two simulations on relatively small lattices at relatively large gluino masses, from which κ_c can be obtained by a linear extrapolation. Proceeding to larger lattices and smaller gluino masses, this estimate can be continuously improved without any further simulations. In this way the interesting range of hopping parameters $\kappa < \kappa_c$ for the investigation of the particle spectrum can be determined.

The values of the gauge coupling parameter β can be fixed by investigating the static potential of an external charge in the fundamental representation and extracting the Sommer scale parameter r_0/a [21], as discussed in Sec. 3. In analogy with QCD, we set the value of r_0 by definition to $r_0 = 0.5$ fm. In this way we can use familiar QCD units for physical dimensionful quantities.

As a measure for the gluino mass we define the dimensionless quantity $M_r \equiv (r_0 m_\pi)^2$, which is expected to be proportional to the gluino mass.

A summary of the simulation parameters is given in Table 1. The simulations are performed on $16^3 \cdot 32$ and $24^3 \cdot 48$ lattices. Extrapolated to κ_c the lattice spacing amounts to $a \simeq 0.097$ fm for the unstout ensembles and $a \simeq 0.088$ fm for the stout ones, see below. The lattice extension $L \simeq 2.1 - 2.3$ fm is expected to be large enough to allow control over finite volume effects on the masses of the bound states.

An issue in lattice simulation is the lightness of the dynamical fermions which leads to slowing down of the update algorithms. The TS-PHMC algorithm turned out to be very efficient in producing short autocorrelations among the gauge configurations. For instance, in the stout-smear runs on a $24^3 \cdot 48$ lattice the integrated autocorrelation of the average plaquette (which belongs to the worst quantities from the point of view of autocorrelations) did always satisfy $\tau_{int}^{plaq} < 10$. The lightest adjoint pion mass in our simulations was about 440 MeV. Simulations for smaller gluino masses and/or finer lattice spacings are going on presently.

3 Static potential and physical scale

Analogy with QCD suggests that the colour charge is confined in SYM, so that the particle states are colour-singlets. Moreover, SYM is expected to confine static quarks as in pure Yang-Mills theory: the static quark-antiquark potential can not be screened by the dynamical gluinos transforming in the adjoint representation, and a non-vanishing string tension arises at large distances.

The numerical results for the static potential $V(r)$ for runs *A–D* are shown in Fig. 1. The linear behaviour at large quark-antiquark separations is compatible with a non-vanishing string tension.

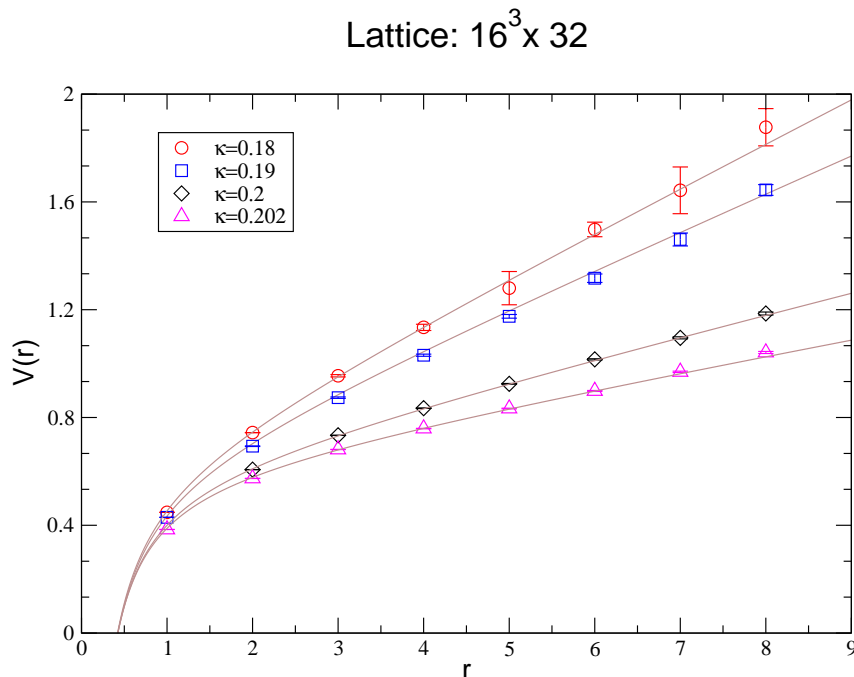


Figure 1: The static quark potential in $\mathcal{N} = 1$ SU(2) SYM. The solid lines are fits to the data.

From the behaviour of the static potential at intermediate distances it is possible to determine the lattice scale, a well-known procedure in lattice QCD. The scale can be

characterised by the Sommer parameter r_0 [21] defined by the relation

$$r_0^2 \left. \frac{dV}{dr} \right|_{r_0} = 1.65. \quad (12)$$

In the SYM model the string tension could in principle also be used to fix the scale, but the Sommer scale parameter is more convenient from the numerical point of view. The numerical results for r_0/a are reported in the sixth column of Table 1. Following the analogous procedure in QCD in a mass independent renormalisation scheme, we extrapolate these data to vanishing adjoint pion mass. For the runs with thin links, where we combine data from the two volumes, we obtain $r_0/a = 5.16(24)$, and for runs with stout links $r_0/a = 5.657(85)$. Using $r_0 = 0.5$ fm this corresponds to $a = 0.097$ fm (thin links) and $a = 0.088$ fm (stout links), respectively. The physical size of the simulated boxes is therefore in these units $L \simeq 1.5 - 2.3$ fm.

4 Spectrum of low-lying bound states

For the investigation of the spectrum of low-lying bound states we concentrate on the operators employed for the construction of the low-energy Lagrangians of [1] and [2]. These are expected to dominate the dynamics of SYM at low energies. Previous experience on the determination of low-lying masses is reported in [8] and [10]. We investigate spin-0 gluino-gluino bilinear operators (adjoint mesons), a spin-1/2 mixed gluino-gluon operator and spin-0 glueball operators. In some cases smearing techniques such as APE [22] and Jacobi smearing [23] are applied in order to increase the overlap of the lattice operator with the low-lying bound state.

4.1 Adjoint mesons

The adjoint mesons are colourless states with spin-parity 0^+ and 0^- , composed of two gluinos. In analogy to flavour singlet states in QCD we denote the former $a\text{-}\eta'$ and the latter $a\text{-}f_0$, where the prefix a indicates ‘‘adjoint’’. The associated projecting operators are the gluino bilinear operators $\mathcal{O}_{\text{meson}} = \bar{\lambda}\Gamma\lambda$ where $\Gamma = 1$ or $\Gamma = \gamma_5$, respectively. The resulting propagator consists of connected and disconnected contributions:

$$\begin{aligned} C(x_0 - y_0) &= C_{\text{conn}}(x_0 - y_0) - C_{\text{disc}}(x_0 - y_0) \\ &= \frac{1}{V_s} \sum_{\vec{x}} \langle \text{Tr}[\Gamma Q_{x,y}^{-1} \Gamma Q_{y,x}^{-1}] \rangle - \frac{1}{2V_s} \sum_{\vec{x}} \langle \text{Tr}[\Gamma Q_{x,x}^{-1}] \text{Tr}[\Gamma Q_{y,y}^{-1}] \rangle, \end{aligned} \quad (13)$$

where $\langle \dots \rangle$ denotes the average over the gauge sample and $V_s = L^3$.

The exponential decay of the connected part defines the adjoint pion mass m_π . This quantity, even if not associated to a physical state of SYM, can be used to determine the gluino mass, as mentioned in Sec. 2. Indeed, according to arguments involving the OZI-approximation of SYM [1], the adjoint pion mass is expected to vanish for a massless gluino and the behaviour $m_\pi^2 \propto m_{\tilde{g}}$ can be assumed for light gluinos [1, 10].

As is well known in simulations of QCD, the numerical evaluation of the disconnected propagators is rather demanding. We employ here two alternative methods, the Stochastic Estimators Technique (SET) in the spin dilution variant [24], and the Improved Volume Source Technique (IVST) [25]. As in QCD, the disconnected diagrams are intrinsically noisier than the connected ones and dominate the level of noise in the total correlator.

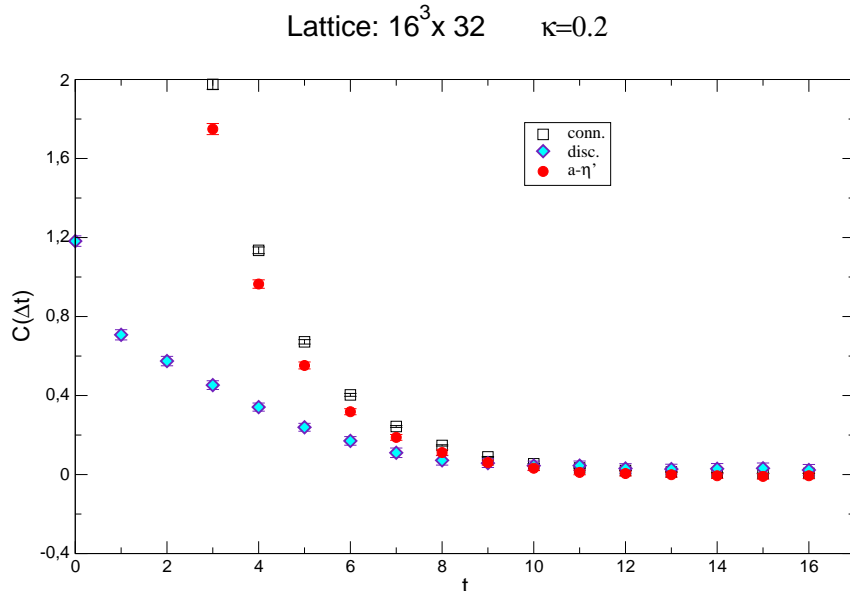


Figure 2: Connected and disconnected pieces and the total time-slice correlation function of the adjoint pseudoscalar $a\text{-}\eta'$.

In the pseudoscalar channel a reasonable signal-to-noise ratio is obtained, allowing the extraction of the mass from the mass fit on most samples. As an example, in Fig. 2 we show the result for the $a\text{-}\eta'$ correlator for run C together with the two different contributions. Examples for the effective masses as a function of the time separation t are shown in Fig. 3

In the scalar channel the extraction of the mass is complicated by the presence of a vacuum expectation value for the projecting operator $\sim \langle \bar{\lambda}\lambda \rangle$. This allowed a relatively precise determination of the $a\text{-}f_0$ mass only for the samples with stout smearing, which give a better signal. Two examples for the effective mass in this channel are shown in Fig. 4. For the future we plan the application of variance reduction techniques for a more precise computation of the disconnected diagrams.

4.2 Scalar glueball

As for the adjoint mesons, we investigated the scalar glueball masses also in both parity channels. In order to improve the signal we applied in this case APE smearing with the variational method [26]. For the positive parity glueball 0^+ we adopted the simplest

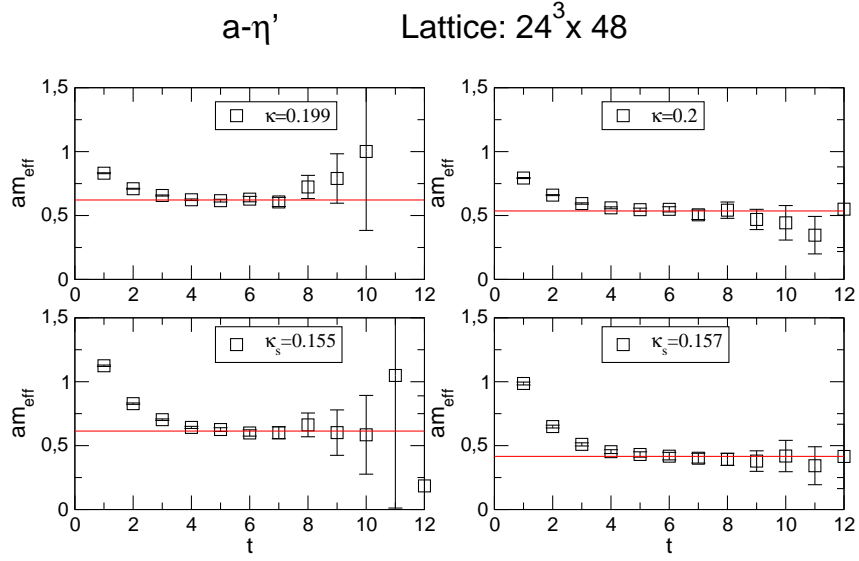


Figure 3: Effective mass of the pseudoscalar $a-\eta'$. The horizontal line represents the result from a one-mass-fit.

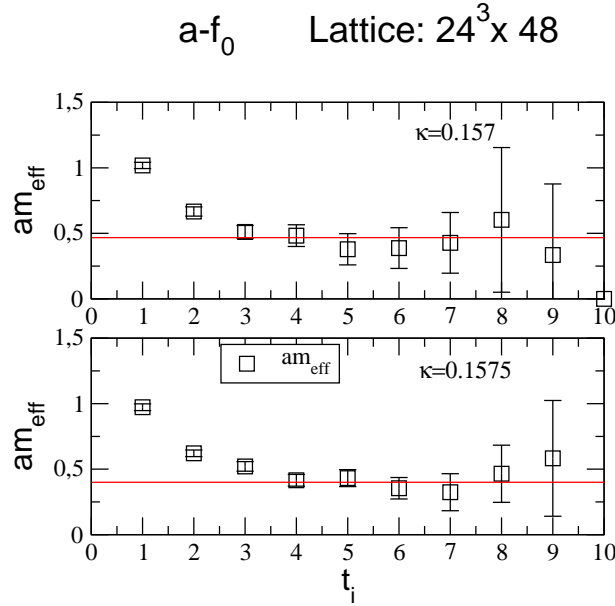


Figure 4: Effective mass of the scalar $a-f_0$. The horizontal line represents the result from a one-mass-fit.

interpolating operator built from space-like plaquettes:

$$\mathcal{O}_{\text{glue},+}(x) = \text{Tr}_c[U_{12}(x) + U_{23}(x) + U_{31}(x)]. \quad (14)$$

For the negative parity state we considered the eight-link operator proposed in [8]. However, the signal obtained in this case was too poor to obtain an estimate of the mass. Therefore we restricted the analysis to the positive parity channel in the following.

Also here, as for the scalar $a-f_0$, the gauge samples generated with stout links generally turn out to give better results for the glueball masses. In Fig. 5 two examples of the effective masses are reported together with the results from one-mass fits with minimal time-distance t_i .

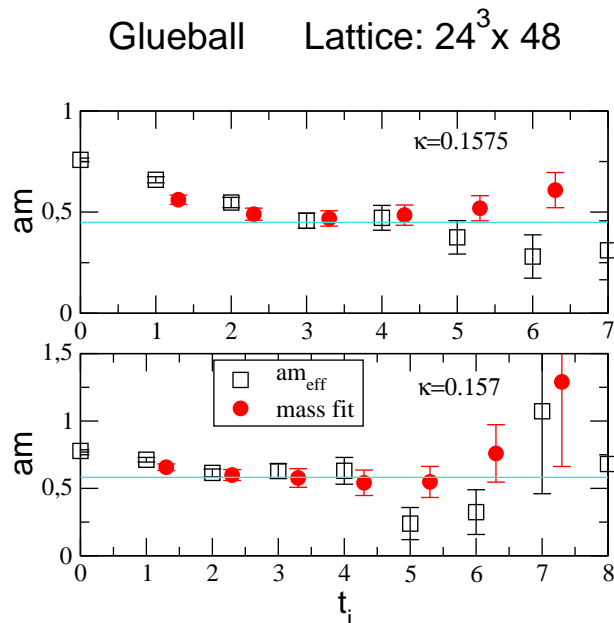


Figure 5: Effective mass and results from one-mass fits for the scalar glueball 0^+ .

4.3 Gluino-glueballs

The gluino-glueballs ($\tilde{g}g$) are spin 1/2 colour singlet states of a gluon and a gluino. They are supposed to complete the Wess-Zumino supermultiplet of the adjoint mesons [1]. For this state we adopt the lattice version of the gluino-gluon operator $\text{Tr}_c[F\sigma\lambda]$ [1], where the field-strength tensor $F_{\mu\nu}(x)$ is replaced by the clover-plaquette operator $P_{\mu\nu}(x)$ [9, 10]:

$$\mathcal{O}_{\tilde{g}g}^\alpha(x) = \sum_{i<j} \sigma_{ij}^{\alpha\beta} \text{Tr}_c[P_{ij}(x)\lambda^\beta(x)]. \quad (15)$$

Here only spatial indices are taken into account in order to avoid links in the time-direction. The clover-plaquette operator, having the correct behaviour under discrete parity and time reversal transformations, is defined as

$$P_{\mu\nu}(x) = \frac{1}{8ig_0} \sum_{i=1}^4 (U_{\mu\nu}^{(i)}(x) - U_{\mu\nu}^{(i)\dagger}(x)) \quad (16)$$

with

$$U_{\mu\nu}^{(1)}(x) = U_\nu^\dagger(x)U_\mu^\dagger(x + \hat{\nu})U_\nu(x + \hat{\mu})U_\mu(x) \quad (17)$$

$$U_{\mu\nu}^{(2)}(x) = U_\mu^\dagger(x)U_\nu(x - \hat{\nu} + \hat{\mu})U_\mu(x - \hat{\nu})U_\nu^\dagger(x - \hat{\nu}) \quad (18)$$

$$U_{\mu\nu}^{(3)}(x) = U_\nu(x - \hat{\nu})U_\nu(x - \hat{\nu} - \hat{\mu})U_\mu^\dagger(x - \hat{\nu} - \hat{\mu})U_\mu^\dagger(x - \hat{\mu}) \quad (19)$$

$$U_{\mu\nu}^{(4)}(x) = U_\mu(x - \hat{\mu})U_\nu^\dagger(x - \hat{\mu})U_\mu^\dagger(x + \hat{\nu} - \hat{\mu})U_\nu(x). \quad (20)$$

The full correlator of the gluino-gluon operator,

$$C_{\tilde{g}g}^{\alpha\beta}(x_0 - y_0) = -\frac{1}{4} \sum_{\vec{x}, \vec{y}} \sum_{i,j,k,l} \langle \sigma_{ij}^{\alpha\alpha'} \text{Tr}[U_{ij}(x)\sigma^a] Q_{x\alpha\alpha', y\beta\beta'}^{-1} \text{Tr}[U_{kl}(y)\sigma^b] \sigma_{kl}^{\beta'\beta} \rangle, \quad (21)$$

is a matrix in Dirac space with two independent components [9]:

$$C_{\tilde{g}g}^{\alpha\beta}(x_0 - y_0) = C_1(x_0 - y_0)\delta^{\alpha\beta} + C_{\gamma_0}(x_0 - y_0)\gamma_0^{\alpha\beta}, \quad (22)$$

with $C_1 = \text{Tr}_D[C_{\tilde{g}g}]/4$ and $C_2 = \text{Tr}_D[\gamma_0 C_{\tilde{g}g}(x)]/4$. We see agreement in the masses extracted from each component, see Fig. 6. For the final estimates we choose the time antisymmetric component C_1 , which appears to provide better plateaus. We apply APE smearing for the links and Jacobi smearing for the fermion fields in order to optimise the signal-to-noise ratio and to obtain an earlier plateau in the effective mass.

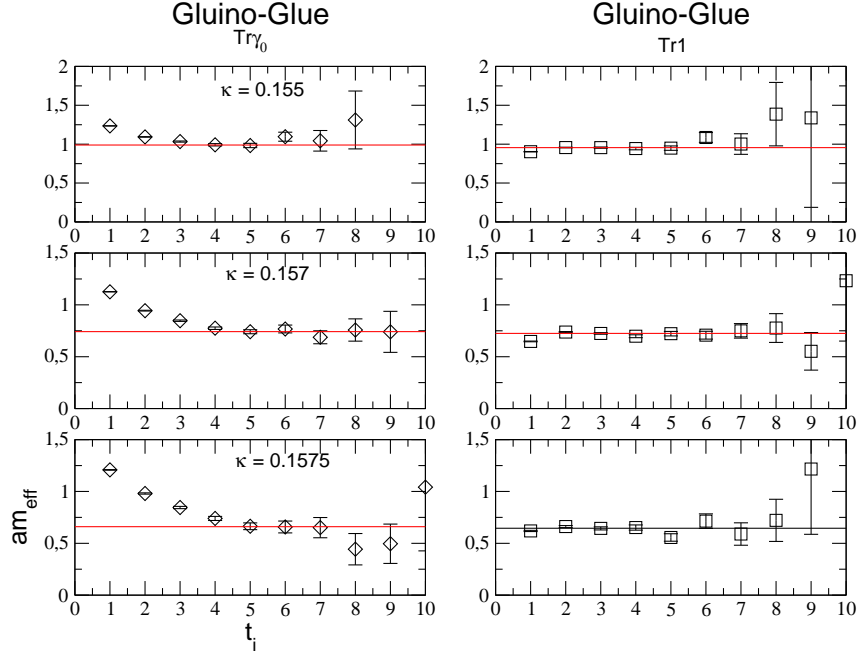


Figure 6: Effective mass of the gluino-gluon operator $\tilde{g}g$.

4.4 Massless gluino limit

Of high interest in lattice simulations of SYM is the point corresponding to a massless gluino, where supersymmetry is expected to emerge in the continuum limit. With Wilson fermions this point must be located by a tuning procedure due to the additive renormalisation of the bare gluino mass.

The subtracted gluino mass can be determined in different ways. It can be directly obtained from the study of lattice SUSY Ward-Identities (WIs) as discussed in [9]. We have implemented the determination of the necessary operators for the WIs. Apart from confirming the smallness of lattice corrections to the WIs, consistent with $\mathcal{O}(a)$ effects, they give results for the gluino mass up to a renormalisation factor. On the other hand, the point of vanishing gluino mass can be estimated in an indirect way from the vanishing of the adjoint pion mass. Indeed, as mentioned above, the pion mass squared $(am_\pi)^2$ is expected to vanish linearly with the (renormalised) gluino mass.

Both the WIs and adjoint pion mass methods give consistent estimates of the critical hopping parameter κ_c corresponding to vanishing gluino mass. As an example, in Fig. 7 we show the the gluino mass and the pion mass squared as a function of $1/\kappa$ for the runs with unstout links on the $24^3 \cdot 48$ lattice. Both clearly show a linear behaviour. The linear extrapolations to vanishing gluino mass give $\kappa_c^{WI} = 0.2027(4)$ from the Ward identities and $\kappa_c^{OZI} = 0.20300(5)$ from the pion mass. Similarly, for the runs with stout links on the $24^3 \cdot 48$ lattice we obtain $\kappa_c^{WI} = 0.15883(85)$ from the Ward identities and $\kappa_c^{OZI} = 0.15793(4)$ from the pion mass, which agree within errors.

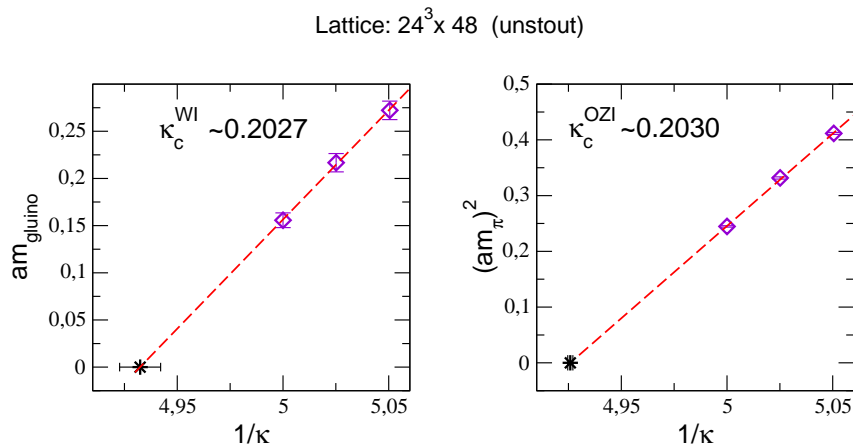


Figure 7: The gluino mass from the SUSY Ward identities (left panel) and the pion mass squared (right panel) as function of the inverse hopping parameter $1/\kappa$. The critical value κ_c is indicated by the asterisk symbol.

5 Spectrum of bound states

The masses of the lightest bound states of low-energy $\mathcal{N} = 1$ SYM determined in this work are collected in Table 2 and a graphic representation is shown in Fig. 8.

Table 2: *Results for the low-lying bound state masses of $\mathcal{N} = 1$ $SU(2)$ SYM from the various runs. The masses are given in lattice units.*

Run	L	κ	$a\text{-}\eta'$	$a\text{-}f_0$	$\tilde{g}g$	glub. 0^{++}
A	16	0.1900	1.3115(67)	2.229(80)	1.862(21)	1.291(13)
B	16	0.1800	1.0396(72)	1.27(18)	1.546(14)	1.156(51)
C	16	0.2000	0.5425(71)	0.931(53)	0.982(10)	0.941(18)
D	16	0.2000	0.361(60)	0.87(10)	0.7532(96)	0.819(19)
\bar{A}	24	0.1980	0.675(18)	1.15(12)	1.1456(82)	
\bar{B}	24	0.1990	0.6215(86)	1.314(32)	1.0789(95)	
\bar{C}	24	0.2000	0.536(24)	0.863(81)	0.9895(70)	0.781(24)
A_s	24	0.1500	1.0114(82)	1.07(16)	1.302(14)	
B_s	24	0.1550	0.614(23)	0.964(70)	0.9559(48)	1.079(92)
C_s	24	0.1570	0.416(29)	0.467(93)	0.7250(56)	0.582(61)
D_s	24	0.1575	0.327(30)	0.351(85)	0.682(30)	0.389(90)

The masses in Fig. 8 are multiplied by the extrapolated value of the Sommer scale parameter and plotted as a function of the squared adjoint pion mass for $(r_0 m_\pi)^2 < 12$. The lightest simulated adjoint pion mass is about 440 MeV in our units. The vertical line in Fig. 8 indicates the massless gluino limit where SUSY restoration is expected up to $\mathcal{O}(a)$ effects. The physical extent of the lattice is 1.5 – 2.3 fm.

The bound state masses appear to be characterised by a linear dependence on $(r_0 m_\pi)^2$, in accordance with the prediction of [27]. An extrapolation of our data with stout links (points B_s to D_s), which have better numerical quality than the unstout ones, to the massless gluino limit yields the numbers in Table 3.

Table 3: *Bound state masses in physical units extrapolated to the massless gluino limit.*

	$a\text{-}\eta'$	$a\text{-}f_0$	$\tilde{g}g$	glub. 0^{++}
m [MeV]	670(63)	571(181)	1386(39)	721(165)

The gluino-glueball ($\tilde{g}g$) with a mass of about 1386 MeV turns out to be considerably heavier than the $a\text{-}\eta'$ with a mass of 670 MeV. Furthermore, the masses of the scalar glueball and the scalar meson $a\text{-}f_0$ are near the mass of the pseudoscalar $a\text{-}\eta'$. The behaviour of scalars is compatible with mixing between 0^+ glueball and $a\text{-}f_0$. The pattern of scalar masses suggests a lower supermultiplet, while the spin-1/2 candidate remains heavier up to the smallest simulated gluino mass in this simulation, and also after extrapolation to κ_c . Whether this outcome is a discretisation artefact or a physical effect, as claimed in [28], should become clear in future studies at finer lattice spacings. As the data at small gluino mass are preliminary, it would be premature to make judgements about this point.

Spectrum of $\mathcal{N}=1$ SU(2) Super-Yang-Mills theory on the lattice

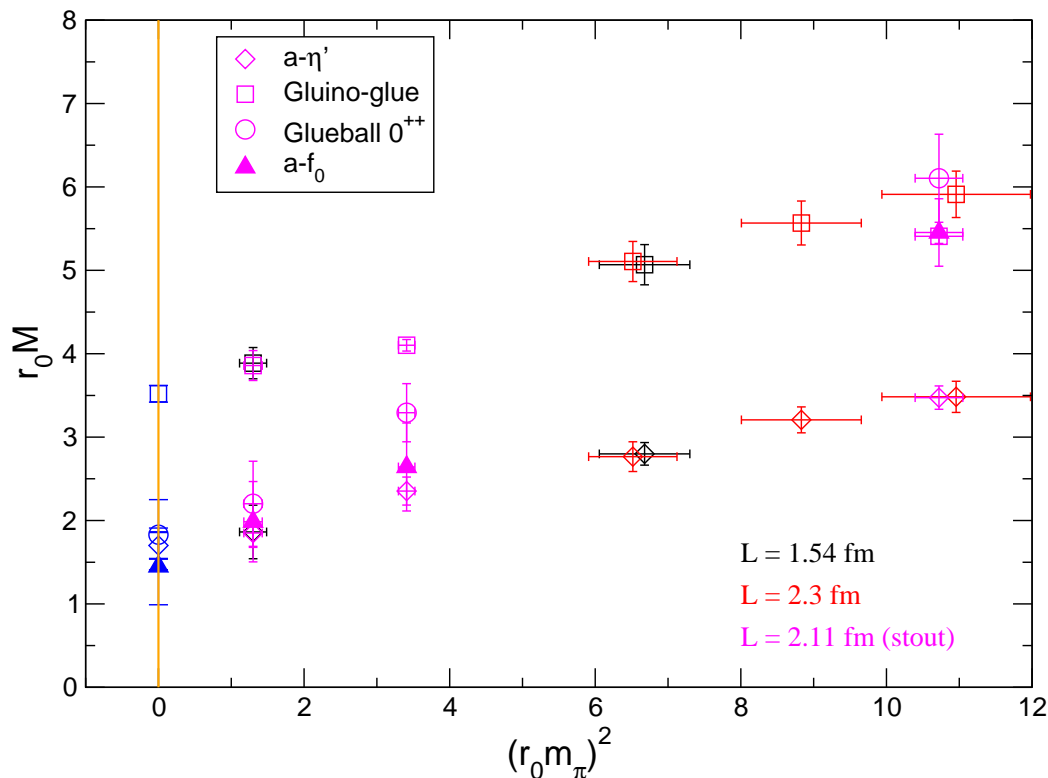


Figure 8: Low-lying bound state masses of $\mathcal{N} = 1$ SU(2) SYM as a function of the adjoint pion mass squared in physical units. The blue symbols represent the extrapolations to the massless gluino limit.

6 Conclusion

In this work first *quantitative* results on the low-energy spectrum of $\mathcal{N} = 1$ supersymmetric Yang-Mills theory are obtained. Physical volumes larger than 2 fm have been simulated, which is the volume usually required for spectrum studies in lattice gauge theory. The comparison of masses on different volumes in otherwise same conditions reveals negligible finite size effects at least for moderate gluino masses. We have collected higher statistics and have used efficient dynamical algorithms such as TS-PHMC, which is suitable for light fermion masses. In addition, the supersymmetric Ward identities and other observables like the confinement potential have been investigated.

From the results of the mass spectrum the question of the gluino-gluino and gluino-gluon mass splitting remains open. It can only be answered by further simulations allowing an extrapolation to the continuum limit.

Acknowledgements

This work has been supported by the German Science Foundation (DFG) under contracts

Mu757/9 and Mu757/13, and by the John von Neumann Institute for Computing (NIC) with grants of computing time. K.D. would like to thank the German Academic Exchange Service (DAAD) for support. The numerical simulations of this work have been performed on the Blue Gene L/P and JuMP systems at JSC Jülich, Opteron PC-cluster at RWTH Aachen and the ZIV PC-cluster of the university of Münster.

References

- [1] G. Veneziano and S. Yankielowicz, Phys. Lett. B **113** (1982) 231.
- [2] G.R. Farrar, G. Gabadadze and M. Schwetz, Phys. Rev. D **58** (1998) 015009.
- [3] A. Armoni, M. Shifman and G. Veneziano, in *From Fields to Strings: Circumnavigating Theoretical Physics*, vol. 1, eds. M. Shifman, A. Vainshtein, J. Wheeler, World Scientific, Singapore, 2005, p. 353; [hep-th/0403071].
- [4] F. Farchioni, G. Münster, T. Sudmann, J. Wuilloud, I. Montvay and E. E. Scholz, PoS(LATTICE 2008) 128, PoS(LATTICE 2007) 135, Eur. Phys. J. C **52** (2007) 305.
- [5] G. Curci and G. Veneziano, Nucl. Phys. B **292** (1987) 555.
- [6] A. Donini, M. Guagnelli, P. Hernandez and A. Vladikas, Nucl. Phys. B **523** (1998) 529.
- [7] I. Montvay, Int. J. Mod. Phys. A **17** (2002) 2377.
- [8] I. Campos, A. Feo, R. Kirchner, S. Luckmann, I. Montvay, G. Münster, K. Spanderen and J. Westphalen, Eur. Phys. J. C **11** (1999) 507.
- [9] F. Farchioni, A. Feo, T. Galla, C. Gebert, R. Kirchner, I. Montvay, G. Münster and A. Vladikas, Eur. Phys. J. C **23** (2002) 719.
- [10] F. Farchioni and R. Peetz, Eur. Phys. J. C **39** (2005) 87.
- [11] K. Demmouche, F. Farchioni, A. Ferling, G. Münster, J. Wuilloud, I. Montvay and E. E. Scholz, PoS(Confinement 2008) 136.
- [12] K. Demmouche, F. Farchioni, A. Ferling, G. Münster, J. Wuilloud, I. Montvay and E. E. Scholz, PoS(LATTICE 2008) 061.
- [13] G.T. Fleming, J. B. Kogut and P. M. Vranas, Phys. Rev. D **64** (2001) 034510.
- [14] M.G. Endres, PoS(LATTICE 2008) 025.
- [15] M.G. Endres, Phys. Rev. D **79** (2009) 094503.
- [16] J. Giedt, R. Brower, S. Catterall, G. T. Fleming and P. Vranas, Phys. Rev. D **79** (2009) 025015.
- [17] I. Montvay, Nucl. Phys. B **466** (1996) 259; Comput. Phys. Commun. **109** (1998) 144.

- [18] I. Montvay and E.E. Scholz, Phys. Lett. B **623** (2005) 73.
- [19] P. Weisz, Nucl. Phys. B **212** (1983) 1;
P. Weisz and R. Wohlert, Nucl. Phys. B **236** (1984) 397 [Erratum-ibid. B **247** (1984) 544].
- [20] C. Morningstar and M.J. Peardon, Phys. Rev. D **69** (2004) 054501.
- [21] R. Sommer, Nucl. Phys. B **411** (1994) 839.
- [22] M. Albanese et al., Phys. Lett. B **192** (1987) 163.
- [23] C. R. Allton et al. [UKQCD Collaboration], Phys. Rev. D **47** (1993) 5128.
- [24] S. J. Dong and K. F. Liu, Phys. Lett. B **328** (1994) 130.
- [25] F. Farchioni, G. Münster and R. Peetz, Eur. Phys. J. C **38** (2004) 329.
- [26] M. Lüscher and U. Wolff, Nucl. Phys. B **339** (1990) 222.
- [27] N. Evans, S. Hsu and M. Schwetz, hep-th/9707260.
- [28] L. Bergamin and P. Minkowski, hep-th/0301155.